Microarrays for biotechnology: The imaging challenge

L.R. van den Doel[a], M.J. Vellekoop[b], P.M. Sarro[b], R. Moerman[c], J. Frank[c], G. van Dedem[c], K.T. Hjelt[b], L.J. van Vliet[a], and I.T. Young[a]

[a]Pattern Recognition Group, Department of Applied Physics
[b]Electron Instrumentation Laboratory, DIMES
[c]Kluyver Laboratory of Biotechnology
Delft University of Technology
NL-2628 CJ Delft, The Netherlands
e-mail: young@ph.tn.tudelft.nl

Abstract: Our goal is to develop intelligent molecular diagnostic systems (IMDS) that can analyze liquid samples that contain a variety of biochemical compounds. In order to analyze the liquid samples we use dedicated microarrays. At this stage, these are basically miniaturized micro titer plates. Typical dimensions of a well are 200 x 200 x 20 μm^3. These dimensions may be varied and the shape of the wells can be modified with a result that the volume of a wells can be from 0.5 to 1.6 nl. For our experiments, we have used wells with the shape of a truncated pyramid. These wells are fabricated in silicon by a wet etching process. For testing purposes the wells are filled with a fluorescing dye (e.g. rhodamine) of various concentrations. To avoid evaporation, glycerol-water 1:1 v/v with a viscosity of 8.3 times the viscosity of water is used as solvent. To analyze the molecular detection capabilities of such a system, we have used an epi-illumination fluorescence microscope equipped with various objectives and a scientific CCD camera to collect the fluorescent light emitted from the solutions in the wells. We have, in particular, studied the effects of lens magnification and numerical aperture, *NA*. on the detection capabilities. From these experiments we have found that for this configuration the detection limit is on the order of nanomolar concentrations of fluorescing particles. This translates to 100,000 molecules per well. Further, we have used the digital analysis of images of the evaporation process to understand how fluorescing particles move during the evaporation process. Using digital images analysis of the interference fringes produced in this dynamic process, we have obtained an axial resolution of 70 water molecules.

Keywords: Microarrays, Fluorescence microscopy, Digital imaging and analysis, Evaporation physics

1. Introduction

One of the most widely exploited fields of research during the last decade is that of combinatorial chemistry. The stated goal of this approach has been to drastically reduce the time and cost that is required to obtain new compounds. Currently, many samples are tested against a large number of targets in microarrays for high-throughput screening. In the future, this technology will lead to a miniaturized lab-on-a-chip. At this moment, however, there are still many challenges to be solved:

- New types of chemistry need to be developed, because the possible targets need to be very sensitive and selective for high-throughput screening.

- Liquid handling needs to be modified to the picoliter range. Ultra small volumes must be fast and automatically dispensed in (sub)-nanoliter wells in an accurate, precise, and reproducible manner.

- A lab-on-a-chip is more than just a miniaturized micro titer plate: microarrays will contain wells with built-in intelligence, that is, integrated actuators and sensors

- Many (fluorescent) signals can be simultaneously generated. Therefore, advanced detectors and detection methods are necessary in order to perform quantitative analysis.

- High-throughput screening generates vast amounts of data. In order to extract useful information, it is essential to develop special data analysis systems. Furthermore, data interpretation systems must be developed to derive new insight into the underlying biochemical principles.

The IMDS program aims to find solutions for the challenges listed above. The goal of this research program is to develop systems that can analyze liquid samples that contain a variety of biochemical compounds such as those associated with environmental testing, agricultural testing, medical diagnostics, drug development and dispensing, consumer products, forensics, and consumer products.

2. Materials

One specific project within this interfaculty research program focuses on a sensor system for the acquisition of the fluorescent signals that will be generated in the wells of the microarrays. Our first approach to develop such a system employs CCD imaging. The design of the microarrays and the liquid handling system will be described in this section.

2.1 Detection system

The experimental setup is built around a Zeiss Axioskop epi-illumination microscope system. This microscope is equipped with a fully automated *xyz*-stage (Ludl Electronics Products Ltd, Hawthorne, NY, USA). A KAF 1400 Photometrics Series 200 CCD camera is mounted on the microscope via a 1.0x camera mount (Diagnostic Instruments Inc., Sterling

Heights, MI, USA). The CCD element consists of 1317 x 1035 pixels with a pixel size of 6.8 x 6.8 μm^2. This CCD camera is Peltier cooled to –42° C. Due to this cooling and a slow readout rate 500 kHz, this camera is photon limited. The characteristics of this camera in terms of Signal-to-Noise Ratio are excellent [1]. A Macintosh computer takes care of the microscope control and the image acquisition. The microscope as well as the camera can be controlled from within the environment of the image processing package SCIL-Image (TNO Institute of Applied Physics (TPD), Delft, The Netherlands, e-mail address: scil@tpd.tno.nl). To image the entire microarray onto the CCD array, a low magnification objective is used: a 2.5x / *NA*=0.075 Zeiss Plan-NEOFLUAR objective. With this objective it is possible to image an area of 3.5 x 2.7 mm^2 onto the CCD array. Using wells with an area of 200 x 200 μm^2 and a center-to-center distance of 300 µm, i.e. there is an empty region of 100 µm between two wells, it is possible to read out 100 wells per image. Wide field-of-view imaging with low magnification optics, however, is at the expense of absolute sensitivity. The reason is that the light-gathering power of an objective lens is proportional to the square of the NA: the lower the NA, the less efficiently photons can be collected [2].

2.2 Design and fabrication of microarrays

Six different types of microarrays have been manufactured at DIMES (Delft Institute for Microelectronics and Submicron Technology, Delft University of Technology, NL-2628 CD Delft, the Netherlands). These wells are fabricated either in silicon or in glass. Different geometries can be made by using different etching mask patterns. For our wells, one mask with circular patterns is used and another mask with square patterns. The dimensions of the patterns are 200 µm in diameter or in width, respectively.

(a) Silicon square wet-etched (b) Silicon circular dry-etched

Fig. 1: *This figure shows two of the six type of wells that have been fabricated. The diameter of the circular masking pattern is 200 µm. The width of the square masking pattern is 200 µm. The depth can vary from 6 µm to 40 µm.*

Both wet and dry etching techniques have been employed on the silicon wafers for the realization of the wells. The wet etching was conducted in potassium hydroxide (KOH). Because of the crystal structure of silicon, this technique results in an *anisotropic* etching of the silicon. Wet etching of the silicon results in wells with the shape of a truncated pyramid, which has <111> planes as side walls for both circular and square etching masks. This type of well is shown in Fig. 1a. The angle of the two planes shown in Fig. 1a—the angle between a <111> plane and a <100> plane—is about 54.7°. The dry etching uses Reactive Ion Etching (RIE) and the wells have a cylindrical or cubic shape after etching with a circular or square masking pattern, respectively. An example is shown in Fig. 1b. Microarrays can also be manufactured in glass resulting in a cylindrical or cubic shape with rounded edges and corners.

One of the microarrays is shown in Fig. 2. Each microarray contains 5 x 5 wells each of which is 200 x 200 x 20 μm^3. The center-to-center distance is 600 µm. The dimensions of the microarray itself are 2 x 1 cm^2.

Fig. 2: *A microarray with 5 x 5 wells*

2.3 Fluid Injection

One of the difficulties involved in the miniaturization of high-throughput screening technologies is liquid handling. Fluid volumes less than a nanoliter need to be injected into small wells. We have used two procedures to fill the wells one manual and one automated.

Manual filling – In the manual procedure, an Eppendorf Transjector 5246 (Eppendorf, Netheler-Hinz GmbH, 22331 Hamburg, GE) is used to inject a small volume of fluid into the wells. (The volumes of the wells described in the previous section ranged from 0.5 nl to 1.6 nl.) The operation of the Transjector is shown in Fig. 3.

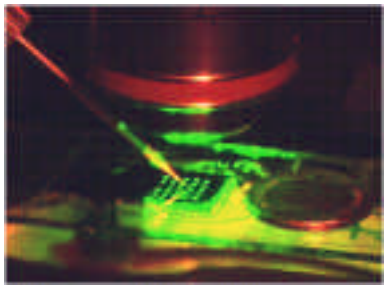

Fig. 3: *The microscope setup for filling the microarrays. The capillary is placed at an angle under the 2.5x microscope objective (working distance 9.3 mm}. The 5 x 5, 200 x 200 µm2 microarray is clearly visible by the scattered excitation light. At the right a "Dutch Dime" 15 mm in diameter is shown to indicate the size.*

Experiments have been done to partially fill the wells, but the variation in the injected volume for a *partially* filled well was quite large. Therefore the wells were always filled completely. The volume variation of a completely filled well—based upon fluorescence intensity measurements—was about 6%.

It is obvious that this kind of liquid handling does not meet our demands. With this device it is only possible to fill a single well at a time with just one liquid sample. We, however, want to fill an entire microarray at once with many different chemicals.

Automated filling – In the automated procedure, we have developed (and patented) a dispensing mechanism based on Electro-Spray Deposition (ESD). By pumping the fluid at rates of about 40 pl/s through a pipette onto a silicon wafer (or into the wells in the wafer) and by placing a voltage of about 1 kV between the pipette and the wafer, a mist of very fine droplets is formed. By controlling the distance between the pipette and the wafer (*z*-axis control), the spray can be turned on and off.

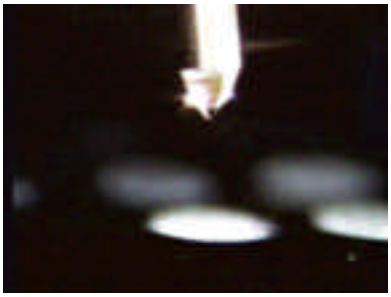

Fig. 4: *Sample deposited by ESD . The tip is about 200 µm above the wafer and the voltage is about 1 kV. The diameter of the deposited sample is 150 µm.*

For the experiments we have used several different solutions of the fluorescing dyes rhodamine and resorufin. In the previous section we indicated that the volume of a well is on the order of one nanoliter. If a droplet of water of this size is pipetted into a well, it evaporates in a few seconds. In order to reduce the evaporation rate we have used solutions of glycerol : water (1:1, v/v) with a viscosity of $8.3\eta_o$, where η_o is the viscosity of water. With this high viscosity the evaporation process of the liquid is extended to more than 45 minutes. To lower the surface tension a detergent is added to the solutions.

The solutions of Rhodamine B (Merck, Ge) were prepared by serial dilution in a glycerol : water (1:1, v/v) mixture containing 0.005\% (w/v) Sarkosyl NL-97 detergent (Cyba-Geigy). This produces a series of solutions with decreasing, known amounts of fluorescent dye. The solutions of Resorufin were also prepared by serial dilution in a glycerol : 50 mM sodium phosphate buffer, pH 7.4 (1:1, v/v) mixture containing 0.005\% (w/v) Sarkosyl NL-97 detergent (Cyba-Geigy).

The result of filling a 5 x 5 array with different concentrations of fluorescent dye is shown in Fig. 5.

3. Experimental results

In this section, we will describe a number of experiments that have been performed with the microarrays. All experiments described below are performed with the wells with the shape of a truncated pyramid (See Fig. 1a.) These wells have dimensions of 200 x 200 x 20 μm^3. This corresponds to a volume of 0.8 nl.

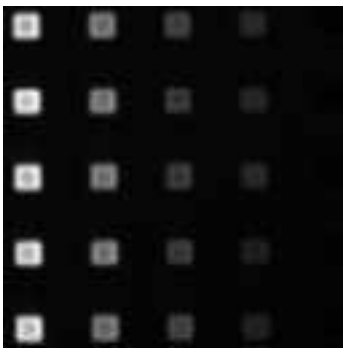

Fig. 5: *5 x 5 array filled with five different Resorufin concentrations (horizontal). Each concentration is repeated five times (vertical).*

3.1 Detection limit

The measured intensity for a well is directly proportional to the number of molecules in the well which, in turn, is directly related to the amount of liquid in the well. To establish the detection limit of our system we examine the total brightness per well averaged over the five "vertical" wells (as shown in Fig. 5) for each of the columns (again, as in Fig. 5) and plot the brightness as a function of fluorescence concentration. As a control the fifth column (on the right) is filled with distilled water that should produce, at most, autofluorescence. The results are shown in Fig. 6.

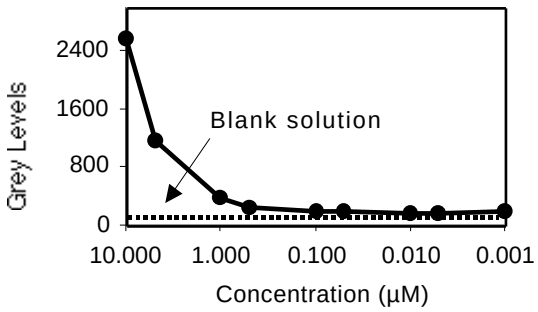

Fig. 6: *Grey value measurements as a function of fluorescence concentration. Note that decreasing concentration is to the right.*

We have defined the detection limit as when the brightness "signal" is about 2σ above the background level which, in this case, is represented by the blank solution. As can be seen in Fig. 6 this is at about the 1 µM concentration. Given the volume associated with the well this corresponds to about 10^8 fluorescing molecules per well.

Note that in this implementation the entire 5 x 5 array is being imaged all at once using the large field-of-view and the low magnification and low *NA* microscope objective. To assess the effects of both

magnification and the NA, we performed two additional experiments where we varied both parameters. The results are shown in Fig. 7.

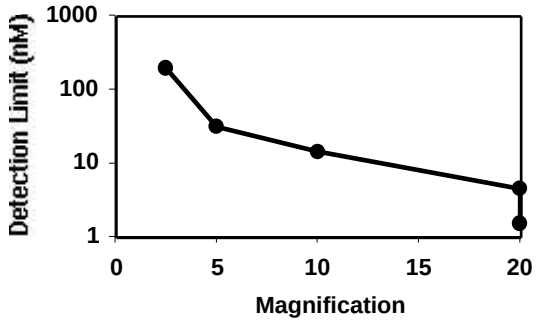

Fig. 7a: *Detection level values as a function of lens magnification.*

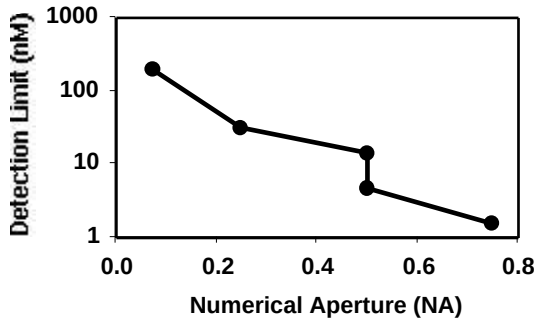

Fig. 7b: *Detection level values as a function of lens numerical aperture, NA.*

These two graphs show that by increasing the magnification and/or the *NA*, we can achieve a detection level of about 1 nM which translates to about 100,000 fluorescing molecules per well. This type of imaging is no longer wide-field but instead involves the sequential analysis of each of the wells.

3.2 Evaporation of solvents

A droplet of water of 1 nl injected into one of the wells evaporates within a few seconds because of its low viscosity. It is important to understand this phenomenon because of the following issues:

· During evaporation there is a liquid flow directed outwards. How does this influence biochemical reactions in the wells?

· What is the relation between the evaporation rates and the sizes and shapes of the wells? Experimental results indicate that the evaporation rate depends linearly on the perimeter of the wells.

· Due to interference in a thin liquid sample, the intensity fluctuates significantly. This effect could hamper our fluorescence quantitation in thin films.

· A model-based study of the evaporation process in sub-nanoliter wells might allow the possibility to investigate shapes of wells that minimize the evaporation rate.

In order to prevent evaporation or at least to slow down this process, we have used solvents with a higher viscosity. We have mixed ethylene-glycol and water in the ratio required to produce a viscosity of about $5\eta_o$. Once a well is filled with this solvent, it evaporates in about 20 minutes. We have monitored this process by acquiring an image every 30 seconds. Four images of this process are shown in Fig. 8.

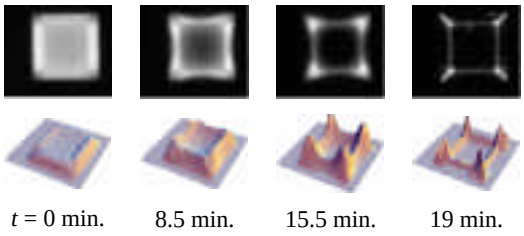

Fig. 8: *A series of images showing the evaporation process of ethylene-glycol and water 90%/10%,v/v in a single well at the indicated times.*

Immediately after injection of the liquid, the intensity signal from the well is uniform except for some geometrical effects along the sidewalls and the corners of the well. After filling the well, the liquid is "pinned" to the edge of the well. During evaporation, the pinning of the liquid ensures that the evaporation from the edge is replenished by liquid from the center part of the liquid in the well [3]. This can be seen qualitatively in Fig. 8: the fluorescent signal gets weaker in the center, until the bottom of the well is reached. The signal disappears from that area sometime between 10 and 15 minutes.

While the evaporation continues, the liquid is “pinned” in the four corners of the well. At these spots the concentration of fluorescing particles is increasing. Finally, when the solvent is completely evaporated, the particles loose their fluorescent behavior and the signal disappears. In Fig. 9 the average fluorescence signal from the total well as well as the signals from the center, from one of the sidewalls, and from one of the corners of the well is shown as a function of time.

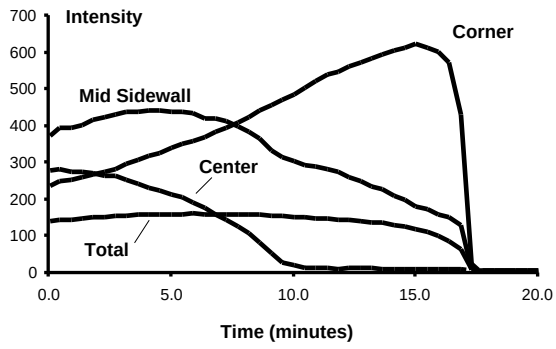

Fig. 9: *The average fluorescence signal from various positions within the well as a function of time.*

As shown in Fig. 9, the average signal of the *entire* well does not decrease during the evaporation process. The slight increase of the signal in the beginning is caused by the geometrical effects. These effects are less than 10% of the signal. Furthermore, it can be seen that the signal in the corners of the well increases steadily because of the accumulation of the fluorescent particles at these spots.

Note that with our microscope system the three dimensional liquid-air interface, the meniscus, is projected onto a two-dimensional image plane. Therefore it is not possible to retrieve the shape of the meniscus during the evaporation. It is, however, possible to monitor this effect with a confocal scanning laser microscope.

4. Confocal and interferometric analysis

When the three-dimensional well filled with a fluorescing solution is analyzed using a sequence of confocal images, an *x-z* display clearly shows the dynamic changes in the meniscus of the fluid. See Fig. 10.

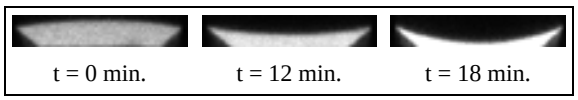

Fig. 10: Evaporation of fluorescent solution viewed through an *x-z* projection of a confocal microscope. Note that the angles of the sides of the well are the 54.7° mentioned earlier.

When we (again) use a conventional fluorescence microscope instead of the confocal version we observe interference fringes that change as a function of time. This is illustrated in Fig. 11 for three frames out of a 20 minute movie.

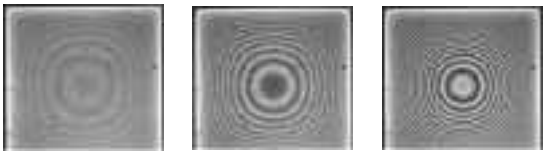

Fig. 11*: Three frames of the acquired image sequence showing the evolving interference pattern*

The interference pattern is caused by the direct part of an incident plane wave interfering with the part of the incident plane wave that is reflected at the bottom of the well. The sum of all these modulations gives rise to the observed interference pattern. The optical path difference (OPD) between the direct part and the reflected part of the incident plane wave at a certain height above the reflecting bottom of the well is proportional to this height. The same holds for the phase difference corresponding to this optical path difference. *This implies that the height of the meniscus can be retrieved if the absolute phase difference can be measured.*

The acquired interferograms can be described by the sum of a space and time varying background, the cosine of the wrapped phase map modulated in amplitude, and an additive noise term. The unwrapped phase map is related to the height of the meniscus level. The goal of the unwrapping algorithm is first to estimate the wrapped phase map from the interferogram and second to unwrap the wrapped phase map. This results in the height profile of the meniscus as a function of space and time. The two steps together are known as an unwrapping algorithm. We unwrap the interferograms in time point by point. This means that there is no spatial correlation between the measured heights of the meniscus at a certain time. The details of the two-step unwrapping procedure can be found in [4]. A typical result of this algorithm is shown in Fig. 12. Digital videos showing these height profiles of the meniscus changing as a function of time are available as well.

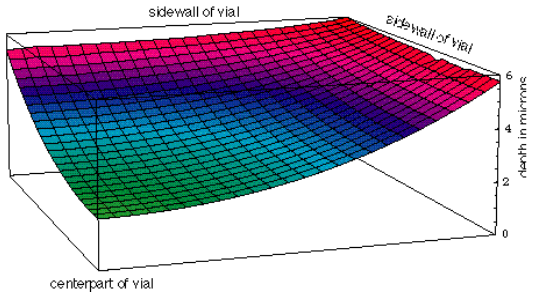

Fig. 12: *Retrieved height profile of the meniscus as computed with the temporal phase unwrapping algorithm*

Using this procedure we can monitor the absolute height of the meniscus as the fluid evaporates from a starting value of 6 µm down to a final value of 0 µm. The resolution of this procedure is about 20 nm which corresponds to about 70 water molecules!

5. Conclusion

In this phase of our research program, we use miniaturized micro titer plates fabricated in silicon. In the future, these microarrays will have integrated intelligence by means of several sensors and actuators. The volume of each well is on the order of one nanoliter. In order to pipette such a small volume, a special technique—electrospray dispensing—has been used. To avoid evaporation, solutions with a high viscosity must be used. We have used both glycerol/water and ethylene-glycol/water to increase the viscosity and thereby decrease the evaporation rate.

To determine the sensitivity we have used an epi-illumination microscope equipped with various magnification optics and a scientific CCD camera. With this setup the detection limit is on the order of nanomolar concentrations. The system can be improved by reducing the amount of stray light, better use of the illumination source, and better light collection efficiency. There are several ways to implement these improvements. One possibility is to separate the *excitation* path from the *emission* path in the optical system. A second possibility is to insert a grating right after the light source. This grating would then pass only the light that reaches the area of the wells and not the inter-well surfaces. A third possibility would be to integrate the light source into the wells. This might be achieved by means of optical waveguides or with light-emitting polymers. Finally,

we will try to integrate detectors into the wells. We will be investigating all these possibilities in the near future.

Our experiments in evaporation physics have shown that understanding of the mechanisms can be useful in designing wells that have optimized properties for mixing of analytes and reagents as well as the detection of fluorescent reaction products.

Acknowledgments

This work has been supported by the Delft Interfaculty Research Center Intelligent Molecular Diagnostic Systems (DIOC-IMDS) and by the FOM Rolling Grants Program.

References

[1] J. C. Mullikin, L. J. Van Vliet, H. Netten, F. R. Boddeke, G. Van der Feltz, and I. T. Young, "Methods for CCD Camera Characterization," presented at SPIE Conference on Image Acquisition and Scientific Imaging Systems, San Jose, California, 1994.

[2] F. Rost, *Fluorescence Microscopy*, vol. 1. Cambridge, England: Cambridge University Press, 1992.

[3] R. Deegan, O. Bakajin, T. Dupont, G. Huber, S. Nagel, and T. Witten, "Capillary flow as the cause of ring stains from dried liquid drops," *Nature*, vol. 389, pp. 827-829, 1997.

[4] L. R. v. d. Doel, L. J. v. Vliet, K. T. Hjelt, M. J. Vellekoop, F. Gromball, J. G. Korvink, and I. T. Young, "Nanometer-scale height measurements in micro-machined picoliter vials based on interference fringe analysis," presented at 15th ICPR, Barcelona Spain, 2000.